

1 **Development of monoclonal antibody-based blocking ELISA for detecting SARS-CoV-2**
2 **exposure in animals**

3

4 Fangfeng Yuan^{1a}, Chi Chen^{1a}, Lina M. Covaleda², Mathias Martins², Jennifer M. Reinhart³,
5 Drew R. Sullivan^{3,4}, Diego G. Diel², Ying Fang^{1*}

6

7 ¹Department of Pathobiology, College of Veterinary Medicine, University of Illinois at
8 Urbana-Champaign, Urbana, IL, USA

9 ²Department of Population Medicine and Diagnostic Sciences, Animal Health Diagnostic
10 Center, College of Veterinary Medicine, Cornell University, Ithaca, NY, USA

11 ³Department of Veterinary Clinical Medicine, College of Veterinary Medicine, University of
12 Illinois at Urbana-Champaign, Urbana, IL, USA

13 ⁴Medical District Veterinary Clinic, College of Veterinary Medicine, University of Illinois at
14 Urbana-Champaign, Chicago, IL, USA

15

16

17

18 ^aThese authors contributed equally.

19

20 *To whom correspondence should be addressed:

21 Email: yingf@illinois.edu (Ying Fang)

22

23

24

25 **ABSTRACT**

26 The global pandemic of severe acute respiratory syndrome coronavirus 2 (SARS-CoV-2)
27 poses a significant threat to public health. Besides humans, SARS-CoV-2 can infect several
28 animal species. Highly sensitive and specific diagnostic reagents and assays are urgently
29 needed for rapid detection and implementation of strategies for prevention and control of the
30 infection in animals. In this study, we initially developed a panel of monoclonal antibodies
31 (mAbs) against SARS-CoV-2 nucleocapsid (N) protein. To detect SARS-CoV-2 antibodies in
32 a broad spectrum of animal species, a mAb-based bELISA was developed. Test validation
33 using a set of animal serum samples with known infection status obtained an optimal
34 percentage of inhibition (PI) cut-off value of 17.6% with diagnostic sensitivity of 97.8% and
35 diagnostic specificity of 98.9%. The assay demonstrates high repeatability as determined by a
36 low coefficient of variation (7.23%, 6.95%, and 5.15%) between-runs, within-run, and
37 within-plate, respectively. Testing of samples collected over time from experimentally
38 infected cats showed that the bELISA was able to detect seroconversion as early as 7 days
39 post-infection. Subsequently, the bELISA was applied for testing pet animals with COVID-
40 19-like symptoms and specific antibody responses were detected in two dogs. The panel of
41 mAbs generated in this study provides a valuable tool for SARS-CoV-2 diagnostics and
42 research. The mAb-based bELISA provides a serological test in aid of COVID-19
43 surveillance in animals.

44

45 **IMPORTANCE**

46 Antibody tests are commonly used as a diagnostic tool for detecting host immune
47 response following infection. Serology (antibody) tests complement nucleic acid assays by
48 providing a history of virus exposure, no matter symptoms developed from infection or the
49 infection was asymptomatic. Serology tests for COVID-19 are in high demand, especially
50 when the vaccines become available. They are important to determine the prevalence of the
51 viral infection in a population and identify individuals who have been infected or vaccinated.
52 ELISA is a simple and practically reliable serological test, which allows high-throughput
53 implementation in surveillance studies. Several COVID-19 ELISA kits are available.
54 However, they are mostly designed for human samples and species-specific secondary
55 antibody is required for indirect ELISA format. This paper describes the development of an
56 all species applicable monoclonal antibody (mAb)-based blocking ELISA to facilitate the
57 detection and surveillance of COVID-19 in animals.

58

59

60 **Keywords:** SARS-CoV-2; nucleocapsid; monoclonal antibody; bELISA; sera-surveillance

61

62 INTRODUCTION

63 The causative agent of Coronavirus Disease 2019 (COVID-19), severe acute respiratory
64 syndrome-related coronavirus 2 (SARS-CoV-2) is a new member of the family *coronaviridae*
65 within the order *Nidovirales* (1). Nidoviruses are a group of positive-stranded RNA viruses,
66 which replicate through a nested 3'-co-terminal set of subgenomic mRNAs, each possessing
67 a common leader and a poly-A tail (2). The coronaviruses have an intriguing distant
68 evolutionary relationship to other members of the order *Nidovirales*, but possess unique
69 characteristics among currently known +RNA viruses. The coronavirus virion has a
70 characteristic crown-like appearance with spike (S), membrane (M) and envelope (E) proteins
71 inserted into the phospholipid-bilayered envelope. Inside the lipid bilayers, the RNA genome
72 is packaged with a nucleocapsid (N) composed of N proteins. The replicase-associated genes,
73 ORF1a and ORF1b, situated at the 5'-end of the viral genome. They encode two large
74 polyproteins, pp1a and pp1ab, which are cleaved by viral encoded proteases to generate 16
75 known functional nonstructural proteins (nsp 1-16). The 3'-end of the viral genome encodes
76 four major structural proteins: S, M, E and N proteins, and several other minor structural and
77 accessory proteins (3). Host antibody responses induced by SARS-CoV-2 infection are
78 mainly directed against S and N proteins (4).

79 SARS-CoV-2 has a broad host range (5). Besides humans, SARS-CoV-2 has been
80 reported to infect multiple animal species, including cat (6), tiger (7), lion (7), snow leopard
81 (8), deer (9), mink (10), dog (11, 12), etc. These findings cause great concerns on the
82 potential for human to animal and animal to human transmission, along with the appearance
83 of viral mutations as the virus spillover between species. Highly sensitive and specific
84 diagnostic reagents and assays are urgently needed for rapid detection and implementation of
85 control and prevention strategies.

86 Current diagnostic assays for SARS-CoV-2 detection mainly target viral nucleic acids or
87 host antibodies against the viral infection. Nucleic acid tests detect active virus replication
88 and shedding, while antibody tests reveal the previous exposure to the virus (13, 14). The fact
89 that SARS-CoV-2 is capable of infecting a diverse range of animal species causes challenges
90 for antibody test development, as certain reagents such as species-specific secondary
91 antibodies are not commercially available for most animal species. Neutralization tests are an
92 option to screen all animal species for SARS-CoV-2 neutralizing antibodies. However, it has
93 limitations for large-scale field surveillance (15, 16). In contrast to the traditional indirect
94 Enzyme-Linked Immunosorbent Assay (iELISA), monoclonal antibody (mAb)-based
95 blocking ELISA (bELISA) is capable of detecting host antibodies independent of species-
96 specific secondary antibody reagents (17). The bELISA was reported to be able to provide
97 similar level of sensitivity as traditional indirect ELISAs, but with higher level of specificity
98 (18). In this study, a panel of mAbs against SARS-CoV-2 N protein was generated, and a
99 mAb #127-3-based bELISA was developed. Subsequently, the bELISA was applied to detect
100 seroconversion in an experimental cat infection study (19) and diagnosis of SARS-CoV-2
101 specific antibody response in dogs from a pet animal clinic.

102

103 RESULTS

104 **Generation and characterization of mAbs against SARS-CoV-2 N protein.** To
105 produce N antigen for mice immunization, synthetic gene of SARS-CoV-2 Wuhan-hu-1
106 strain was cloned and expressed as a His-tagged recombinant protein. On SDS-PAGE
107 analysis, the purified N protein showed a single band with predicted molecular mass around
108 47.4 kDa (Figure 1A). The identity of the recombinant N protein was further confirmed on
109 western blot using anti-His-tag antibody (Figure 1A).

110 To generate the SARS-CoV-2 specific mAbs, mice were immunized with N antigen.
111 After the fusion of mice splenocytes with myeloma cells, supernatants from the resulting
112 hybridoma cells were screened by IFA using transfected MARC-145 cells expressing N
113 protein. A total of 4 mAbs (clone #41-10, 86-12, 109-33, 127-3) were obtained. One
114 additional mAb B6G11 previously developed in Diel's lab (20) was included in the analysis.
115 IFA result showed that all 5 mAbs recognized N proteins expressed in MARC-145 cells
116 (Figure 1B). Using the cell lysate of transfected 293T cells that express N protein, this panel
117 of mAbs was determined to be able to detect the N protein by western blot and
118 immunoprecipitation (IP) (Figure 1C). To further determine if this panel of mAbs recognizes
119 the N protein in virus-infected cells, Vero cells infected with SARS-CoV-2 variants,
120 including B.1, WA1, P.1, B.1.1.7, and B.1.617.2, were subjected to IFA. The results showed
121 that this panel of mAbs had different levels of reactivity with each of the variant, of which the
122 mAb #127-3 and B61G11 had strong reactivity, #41-10 and #86-12 had moderate reactivity,
123 while #109-33 had weak reactivity (Table 1).

124 The mAb cross-reactivity with other common coronaviruses was further evaluated. We
125 tested N proteins of common coronaviruses from SARS-CoV-2 susceptible host species,
126 including the four human coronaviruses, two feline coronaviruses, two canine coronaviruses,
127 mink and ferret coronaviruses (Table 2). Flag-tagged N proteins from each of these viruses
128 were expressed in transfected cells. IFA results showed that mAb #86-12 can cross-react with
129 the N protein of SARS-CoV, HCoV-OC43, and CCoV-Type 1, while mAb #B61G11 can
130 cross-react with the N protein of SARS-CoV. In contrast, mAb #41-10, #109-33, and #127-3
131 did not cross-react with any of the N proteins from corresponding coronaviruses.

132 **Development and validation of #127-3 mAb-based bELISA.** In order to detect anti-N
133 antibody response in multiple animal species (independent of species-specific reagents), we
134 further developed a mAb-based bELISA. Since mAb #127-3 had strong reactivity with
135 different SARS-CoV-2 variants, and this mAb did not cross react with the other common
136 coronaviruses and SARS-CoV-1, mAb #127-3 was selected for the assay development.

137 *Establishment of serum standards.* Initially, a set of internal control serum standards
138 were established using cat sera collected from our previous study (19). A group of 24 cats
139 were experimentally infected with SARS-CoV-2 virus (D614G, Delta, and Omicron). Serum
140 samples collected from the cats at 14 days post infection were pooled into a single lot of
141 positive control serum. Similarly, large quantities of the known negative cat sera was pooled
142 into a single lot of negative control serum. The positive control standards were set as three
143 levels in the indirect ELISA, including high-positive (OD of 1.5-2.0), medium-positive (OD

144 of 1.0-1.5), and low-positive (OD of 0.8-1.0), while the negative control standard generated
145 an OD of less than 0.3 in the indirect ELISA (Figure 2A). Using the positive and negative
146 control standards, bELISA conditions were optimized by checkerboard titration of the antigen
147 (N protein), biotinylated mAb #127-3, HRP-conjugated streptavidin, blocking and sample
148 buffer component, incubation temperature and time, etc. With the optimized test conditions,
149 the bELISA generated percentage of inhibition (PI) value 75-85% for high-positive standard,
150 55-65% for medium-positive standard, 35-45% for low-positive standard, and approximate
151 0% for negative control standard (Figure 2B).

152 *Analytical sensitivity of bELISA.* Analytical sensitivity of the bELISA was determined by
153 using the high-positive and negative control standards. Standard sera were titrated with two-
154 fold serial dilutions in triplicate. As shown in Figure 3, a dilution of 1:128 was the highest
155 dilution that generates a statistical difference ($p < 0.01$) between the positive and negative
156 control standards. A 1:4 dilution of the sample was selected for the bELISA, as it maximized
157 the discrimination between positive and negative results and minimized background
158 interference.

159 *Diagnostic sensitivity and specificity of bELISA.* To evaluate the diagnostic sensitivity
160 and specificity of the mAb-based bELISA, a panel of serum samples with known antibody
161 status was tested, including 45 positives and 88 negatives collected from cat, ferret, mink, and
162 deer. Before testing in bELISA, all serum samples were analyzed by serum neutralization
163 assay to confirm the antibody status. The bELISA result showed that a cut-off PI value of
164 17.60% produced a maximized diagnostic sensitivity of 97.8% (95% confidence interval:
165 88.2-99.9%) and diagnostic specificity of 98.9% (95% confidence interval: 93.8-100%)
166 (Figure 4A). Subsequently, a single-graph ROC analysis was conducted by comparing false-
167 positives ($1 - \text{diagnostic specificity}$) and true-positives (diagnostic sensitivity). The area
168 under the curve (AUC) represents the overall accuracy of the test. An AUC of 1 indicates a
169 perfect test, and above 0.9 indicates high accuracy. The AUC of #127-3 mAb-based bELISA
170 was 0.998 ($p < 0.001$) with a 95% confidence interval of 97%–100%, demonstrating the high
171 accuracy of the assay (Figure 4B).

172 *Repeatability of bELISA.* Repeatability determines the ability of an assay to produce
173 similar results from multiple preparations and runs of a same sample. In this study,
174 repeatability of #127-3 mAb-based bELISA was assessed by running a single lot of medium-
175 positive control serum standard. The percentage of coefficient of variation (% CV) was
176 calculated to measure the repeatability. The results showed that within plate % CV was
177 5.15% (mean value of 55.37% \pm standard deviation of 2.84%), between-plate % CV within
178 one run was 6.95% (mean value of 55.37% \pm standard deviation of 3.85), while the between
179 runs % CV was 7.23% (mean value of 55.37% \pm standard deviation of 4%). The values of %
180 CV below 10% indicate that the #127-3 mAb-based bELISA is highly repeatable (18, 21).

181 **Detection of seroconversions in SARS-CoV-2 infected cats.** Next, we applied the
182 bELISA to investigate the dynamics of anti-N antibody response in SARS-CoV-2 infected
183 cats. Serum samples were collected from our previous study (19), in which 3 groups of cats
184 ($n = 8$) were experimentally inoculated with each of the SARS-CoV-2 variants (B.1, Delta,

185 Omicron). Serum samples were collected at 0, 3, 5, 7 and 14 days post infection. This set of
186 samples was tested by bELISA and results showed that anti-N antibody response was
187 detected as early as 7 dpi for B.1 and Delta variants, then dramatically increased to a high
188 level (PI = 47.03% for B.1, PI = 71.42% for Delta variant) at 14 dpi (Figure 5A). Omicron
189 variant-induced antibody response (PI = 27.87%) was detected at a late time point (14 dpi).
190 Overall, Delta variant induced the highest antibody response compared to B.1 and Omicron
191 variants. This result is consistent with that of virus neutralization assay. The same trend of
192 dynamics was also observed for serum neutralizing activities against the live virus of Delta
193 variant (B.1.617.2) using the same set of serum samples (Figure 5B).

194 **Application of bELISA in pet animals with clinical diseases.** We further applied the
195 bELISA for detection of SARS-CoV-2 infection in pet animals. Serum samples were
196 collected from three dogs in a pet clinic. These dogs were experiencing clinical signs of
197 respiratory diseases. The bELISA result showed that two dogs (Dog-1 and Dog-2) were
198 positive for SARS-CoV-2 antibodies with PI values of 18.66% and 46.33% respectively,
199 while the third dog was negative for specific anti-N antibody with a PI value of 2.54%
200 (Figure 6A). The result was further confirmed by serum neutralizing test at USDA NVSL
201 laboratory. The result showed neutralizing titers of 92.86%, 37.04%, and 5.69% for dog 1, 2,
202 3, respectively (Figure 6A). Dog-2 exhibited long-term illness, and returned back to the pet
203 clinic periodically. Serum samples were collected from this dog during each examination in
204 the clinic from February to August, 2022. The bELISA detected the increased antibody titer
205 in 15 days (February 22nd, 2022; PI = 77.54%) after the first examination (February 7th, 2022;
206 PI = 46.33%). The titer was decreased at the third examination (March 10th, 2022; PI =
207 48.45%). At the fourth examination (August 2nd, 2022), 176 days from the first examination,
208 lower level of antibody titer (PI = 31.15%) was still detected (Figure 6B).

209

210 **DISCUSSION**

211 The COVID-19 pandemic has emphasized the critical role of effective diagnostics in the
212 response to outbreaks. Diagnostic tools for active surveillance and monitoring of SARS-CoV-
213 2 are essential for the successful control of the pandemic. Reverse zoonotic transmission of
214 this virus from animals to humans has also been reported, which highlights the need for
215 accurate diagnostic tools to be used at the human-animal interface (22-24). Sera-based
216 diagnostics applicable for large-scale field surveillance in all animal species becomes
217 important to understand mechanism of zoonotic transmission. MAbs are key reagents for
218 detection of viral infections and study the viral pathogenesis. Therefore, the goal of this study
219 was to produce a panel of mAbs against SARS-CoV-2 N protein and develop a mAb-based
220 bELISA for sera-surveillance in an animal species-independent manner.

221 Utilizing hybridoma technology, a panel of mAbs recognizing different epitopes of
222 SARS-CoV-2 N protein was generated. It allows us to select the suitable mAb for bELISA
223 development. The mAb #127-3 was characterized to have strong reactivity in cells infected
224 by different SARS-CoV-2 variants. It did not cross-react with the N protein of other
225 human/animal coronaviruses that we tested, which contributes to the high specificity of the

226 mAb-based bELISA developed thereafter. Due to the unique design of bELISA, high
227 specificity is expected as reported previously for assays targeting African swine fever virus
228 (21) and porcine reproductive and respiratory syndrome virus (18). Our mAb-based bELISA
229 achieved high sensitivity (97.8%) and specificity (98.9%), which is comparable to the current
230 commercially available serological tests. The Abbott assay (SARS-CoV-2 IgG assay, Abbott,
231 Chicago, IL, US) was reported to reach 92.7% sensitivity and 99.9% specificity, the DiaSorin
232 assay (LIAISON SARS-CoV-2 S1/S2 IgG, DiaSorin, Saluggia, Italy) has 96.2% sensitivity
233 and 98.9% specificity, and the Roche assay (Elecsys Anti-SARS-CoV-2 assay, Roche, Basel,
234 Switzerland) has 97.2% sensitivity and 99.8% specificity in human serum samples (25).
235 Similarly, the SARS-CoV-2 surrogate neutralization test achieves 96% sensitivity and
236 99.93% specificity (26). Much higher sensitivity can be achieved in symptomatic individuals
237 and those in the late phase of infection due to robust production of antibody responses (27).

238 Current available serological assays for SARS-CoV-2, include ELISAs, are targeting
239 host antibody response against N or S protein, and most of them are specifically designed for
240 human samples. For example, the Abbott and Roche assays target N protein, while the
241 DiaSorin assay targets S protein. They all primarily are designed for testing human samples
242 and require species-specific secondary antibodies for testing the samples from a specific
243 animal species (25). Notably, the surrogate neutralization test adapted the ELISA format to
244 block bindings between coating ACE2 receptor and HRP conjugated Spike/RBD proteins,
245 which is a cell- and virus-free assay and capable of screening serum samples from all host
246 species (16). However, measuring neutralizing antibodies has to accommodate different
247 variants, since frequent mutations in S protein leads to potential mis-binding of ACE2 and S
248 protein. The mAb-based bELISA developed in this study targets N protein, which is highly
249 conserved across different variants of SARS-CoV-2, thus has less probability to be affected
250 by emerging variants. In addition, due to the abundant presence of N protein, immunoassays
251 targeting N protein are more sensitive than that targeting S protein, especially during the early
252 infection stage (28-31). Previous studies showed that serum SARS-CoV-2 N protein could be
253 a diagnostic marker for detection of early infections (32-34). In the case of SARS
254 coronavirus, N protein could be detected in serum samples from 95% SARS patients at just 3
255 days after symptom onset (35). Consistently, our bELISA was able to detect antibodies
256 against B.1 and Delta variants in cats at 7 days post infection. Furthermore, in combination
257 with an S protein-based test, the N protein-based bELISA is capable of differentiating
258 between infected and vaccinated animals when an S protein-based COVID-19 vaccine is
259 used.

260 We further applied the bELISA to diagnose pet animals with clinical illness. Two dogs
261 were tested positive on the bELISA and results were further confirmed by virus neutralizing
262 assays. Oropharyngeal samples were further collected from both dogs and quantitative RT-
263 PCR was conducted by the USDA NVSL laboratory. The result showed that CT value of
264 Dog-1 was 37.66 with N1 primer set and negative with N2 primer set, while CT value of
265 Dog-2 was 31.32 with N1 primer set and 33.99 with N2 primer set for SARS-CoV-2 nucleic
266 acid detection. These results fall into “suspect” category according to CDC guidelines (36).
267 The owner of Dog-1 was diagnosed as COVID-19 positive in January 2022, suggesting that

268 the dog might have been exposed to the SARS-CoV-2 from the owner and subsequently
269 developed the specific antibody response. The samples that we tested were collected in early
270 February 2022, which might have been about 2-3 weeks after potential exposure to the virus.
271 At this stage, the animal should have already passed the peak time for shedding the virus and
272 developed specific immune response against the viral infection (37). This could explain our
273 observation of a “suspect” level of nucleic acid detected in RT-PCR test, but high level of
274 antibody detected in bELISA and virus neutralizing test. Interestingly, antibody response in
275 Dog-2 lasted for about 6 months. This result is consistent with previous findings in humans,
276 in which a longitudinal analysis of antibody dynamics in COVID-19 convalescents
277 demonstrated that both neutralizing and non-neutralizing antibodies can still be detected over
278 8 months post-symptom onset, although the titer was substantially decreased (38-40).

279 In summary, the panel of mAbs generated in this study provides valuable reagents for
280 disease diagnostics and viral pathogenesis studies. The mAb-based bELISA could be a useful
281 tool for field surveillance to determine the prevalence of COVID-19 in animal populations
282 and identify potential new animal reservoirs.

283

284 MATERIALS AND METHODS

285 **Cells, viruses, and viral genes.** Vero-E6 and MARC-145 cells were maintained in
286 minimum essential medium (Thermo Fisher Scientific, Waltham, MA) supplemented with
287 10% heat-inactivated fetal bovine serum (Sigma-Aldrich, Burlington, MA) and antibiotics
288 (100 µg/mL streptomycin, 100 U/mL penicillin, and 0.25 µg/mL fungizone) at 37°C with 5%
289 CO₂.

290 The SARS-CoV-2 isolates used in this study were obtained from residual de-identified
291 human anterior nares or nasopharyngeal secretions (Institutional review board [IRB] at
292 Cayuga Health System [protocol 0420EP] and Cornell University [protocol 2101010049]).
293 The SARS-CoV-2 D614G (B.1 lineage) New York-Ithaca 67-20 (NYI67-20), Alpha (B.1.1.7)
294 New York City 853-21 (NYC853-21), and Delta (B.1.617.2 lineage) NYI31-21 isolates, were
295 propagated in Vero E6/TMPRSS2 cells, whereas the Omicron BA.1.1 (B.1.1.529) NYI45-21
296 isolate was propagated in Vero E6 cells in BSL3 laboratory conditions at the Animal Health
297 Diagnostic Center (AHDC) Research Suite at Cornell University. The SARS-CoV-2 full-
298 length N gene of Wuhan-hu-1 isolate (GenBank # NC 045512.2) was synthesized (GenScript,
299 Piscataway, NJ) and cloned in the pET-28a (+) vector (Novagen, Madison, WI) or pCAGGS
300 vector (provided by Dr. Adolfo Garcia-Sastre at the Icahn School of Medicine at Mount Sinai
301 in New York City) (41). In addition, N genes of common coronaviruses that infect SARS-
302 CoV-2 susceptible animal hosts were synthesized. Each synthetic gene was fused with a Flag
303 tag (DYKDDDDK) at its C terminus and cloned into a plasmid vector pTwist-CMV-
304 BetaGlobin (Twist Bioscience, San Francisco, CA). The synthesized genes were derived from
305 human coronavirus OC43 (HCoV-OC43; GenBank ID, AY585228.1), human coronavirus
306 NL63 (HCoV-NL63; GenBank ID, AY567487.2), human coronavirus 229E (HCoV-229E;
307 GenBank ID, NC_002645.1), human coronavirus HKU1 (HCoV-HKU1; GenBank ID,
308 NC_006577.2), severe acute respiratory syndrome coronavirus (SARS-CoV; GenBank ID,

309 AY278741.1), middle east respiratory syndrome coronavirus (MERS-CoV; GenBank ID,
310 NC_019843.3), feline infectious peritonitis virus (FIPV; GenBank ID, AY994055.1), feline
311 coronavirus (FCoV; GenBank ID, EU186072.1), canine coronavirus type I (CCoV-type I;
312 GenBank ID, KP849472.1), canine coronavirus type II (CCoV-type II; GenBank ID,
313 KC175340.1), ferret systemic coronavirus (FRSCV; GenBank ID, GU338456.1), and mink
314 coronavirus (MCoV; GenBank ID, HM245925.1).

315 **Recombinant protein preparation.** Recombinant N protein of SARS-CoV-2 was
316 expressed in BL21 *E.coli* as a polyhistidine (6x His-tagged) fused protein. The antigen was
317 produced and purified by following a method described in our previous study (18). Purified
318 proteins were dialyzed using 1x phosphate-buffered saline (PBS) solution under 4°C for three
319 times and then concentrated by polyethylene glycol 8000 (Thermo Fisher Scientific,
320 Waltham, MA).

321 **Monoclonal antibody (mAb) production.** BALB/c mice were immunized with
322 recombinant N protein at a dose of 50-100 µg per mouse and further boosted 2-3 times at an
323 interval of two to three weeks. At three days after the final boost, mice splenocytes were
324 collected and fused with NS-1 myeloma cells to generate hybridoma cells. Specific anti-N
325 antibody-secreting hybridomas were screened by using immunofluorescent assays (see
326 below). Selected hybridomas were expanded in large tissue culture flask. Cell culture
327 supernatants containing specific anti-N mAb were harvested and concentrated using Pierce™
328 Saturated Ammonium Sulfate Solution (Thermo Fisher Scientific, Waltham, MA).
329 Biotinylation of the mAb was performed using a Biotin Conjugation Kit by following the
330 manufacturer's instruction (Abcam, Cambridge, MA). The SARS-CoV-2 N-specific mAb
331 B6G11 was previously developed in Diel lab (20).

332 **Immunofluorescent assay (IFA).** For screening hybridomas and performing antibody
333 cross-reactivity test with other coronaviruses, MARC-145 cells were seeded in 96-well cell
334 culture plates and transfected with plasmid DNA expressing N protein of the corresponding
335 coronavirus. Transfection was performed using TransIT®-LT1 Transfection Reagent (Mirus
336 Bio, Madison, WI). At 48 hours post transfection, cells were fixed with 80% acetone (Thermo
337 Fisher Scientific, Waltham, MA) for 10 min at room temperature. Cell monolayers were
338 incubated with the primary mAb at 37°C for 1 hour, followed by incubation with the
339 secondary antibody, Alexa Fluor 488 AffiniPure goat anti-mouse IgG (H+L) (Jackson
340 Immuno Research, West Grove, PA). Immunofluorescent signals were visualized with an
341 inverted immunofluorescent microscope (LMI6000, LAXCO, Mill Creek, WA). To confirm
342 the reactivity and specificity of the anti-N mAb, Vero E6 Cells were infected with different
343 SARS-CoV-2 variants. At 24 hours post infection, cells were fixed with 3.7% formaldehyde
344 solution in PBS for 30 min followed by permeabilization with 0.1% Triton-X-100 in PBS for
345 10 min at room temperature. After 3 consecutive washing steps with PBS, anti-SARS-CoV-2
346 mAbs diluted in blocking solution (1% BSA in PBS) were added to the cells and incubated
347 for 1 hour at 37 °C in a humidified chamber. Cells were washed again and incubated under
348 the same conditions with goat anti-mouse IgG AlexaFluor 594. Cell nuclei were stained with
349 DAPI and image acquisition was performed with an inverted immunofluorescent microscope.

350 **Western blot.** MARC-145 cells were transfected with plasmid DNA of pCAGGS-N that
351 contains SARS-CoV-2 full-length N gene. At 48 hours post transfection, cells were harvested
352 with Pierce™ IP Lysis Buffer (Thermo Fisher Scientific, Waltham, MA) containing Protease
353 Inhibitor Cocktail (Sigma-Aldrich, St. Louis, MO). Western blot analysis was performed
354 using the method as we described previously (21). The membrane was probed with specific
355 anti-N mAb as the primary antibody and detected by IRDye 800CW goat anti-mouse IgG
356 (H+L) (Li-Cor Biosciences, Lincoln, NE) as the secondary antibody. Protein blots were
357 imaged using an Odyssey Fc imaging system (Li-Cor Biosciences, Lincoln, NE).

358 **Immunoprecipitation.** MARC-145 cells transfected with the recombinant pCAGGS-N
359 plasmid were lysed in Pierce™ IP Lysis Buffer (Thermo Fisher Scientific, Waltham, MA),
360 and then mixed with each of the purified anti-N mAbs. Immune-complexes were precipitated
361 by Protein A/G magnetic beads (Thermo Fisher Scientific, Waltham, MA). Precipitated
362 proteins were separated by SDS-PAGE and analyzed by Western blot as described previously
363 (42).

364 **Serum neutralization test.** Serum neutralization (SN) assay was performed under BSL-3
365 laboratory conditions at Cornell University. Two-fold serial dilutions (1:8 to 1:1024) of cat
366 serum samples were incubated with SARS-CoV-2 Delta variant (B.1.617.2) (100-200
367 TCID₅₀/well) for 1 hour at 37°C. Following incubation of serum and virus, 50 µL of a cell
368 suspension of Vero E6 cells was added to each well of a 96-well plate and incubated for 48
369 hours at 37°C with 5% CO₂. Cells were fixed and subjected to IFA as previously described
370 previously (19). The neutralizing antibody titer was calculated as the reciprocal of the highest
371 serum dilution that generated 100% neutralization of SARS-CoV-2 infection. Samples with
372 antibody titer less than 1:8 were considered as negative.

373 The surrogate virus neutralization test (sVNT) was performed at USDA National
374 Veterinary Services Laboratory (NVSL) at Ames, Iowa. A cPass™ SARS-CoV-2
375 Neutralization Antibody Detection Kit (GenScript, Piscataway, NJ) was used and the test was
376 performed following the instructions of the manufacture. Briefly, 10 µL of serum sample was
377 diluted with 90 µL of sample dilution buffer, followed by taking 60 µL of diluted sample to
378 react with 60 µL HRP-conjugated RBD solution. The mixture of sample and HRP-RBD was
379 incubated at 37°C for 30 minutes. The incubated mixture (100 µL) was added to the plate
380 wells that were pre-coated with hACE2 antigen and then incubate at 37°C for 15 minutes.
381 Wells were washed for three times, followed by addition of 100 µL TMB Solution to each
382 well and incubation in dark at room temperature for 15 minutes. Finally, 50 µL of Stop
383 Solution was added to each well and plate was read at 450 nm using a spectrophotometer.
384 The percent signal inhibition for detecting neutralizing antibodies were calculated and the
385 sample was determined as neutralizing antibody positive if the percent signal inhibition was
386 more than 30%.

387 **Sample sources.** The control serum standards used for ELISAs were created using serum
388 samples collected from our previous cat experiment (19). The positive control serum was
389 collected from cats that were experimentally inoculated with SARS-CoV-2 D614G (B.1),
390 Delta (B.1.617.2), or Omicron (B.1.1.529) variant at 14 days post infection (dpi), while the

391 negative control serum was collected from negative control cats. Large quantities of positive
392 sera were pooled into a single lot of positive control serum, and large quantities of the
393 negative sera were pooled into a single lot of negative control serum. The high-, medium-,
394 and low-positive control serum standards were created by spiking the positive control serum
395 into the negative control serum to generate the desired antibody titers in the ELISAs.

396 For assay validation, four sets of animal serum samples with known infection status were
397 used. The first set contained 17 positive and 43 negative serum samples collected from cats
398 infected with SARS-CoV-2 D614G (B.1), Delta (B.1.617.2), or Omicron (B.1.1.529) strain in
399 study described previously (19). The second set contained 10 positive and 37 negative serum
400 samples collected from SARS-CoV-2 isolate NYI67-20 (B.1 lineage) infected ferrets (43).
401 The third set contained 5 positive and 8 negative serum samples collected from SARS-CoV-2
402 (lineage B) infected deer (44). The fourth set included 13 positive mink serum samples. The
403 antibody status of all the serum samples used for bELISA validation was confirmed by serum
404 neutralizing assay as described above.

405 The capability of the bELISA to detect the seroconversion was evaluated using samples
406 collected from a cat experiment that we reported previously (19). Serum samples were
407 collected at 0, 3, 5, 7, 14 days post infection (dpi).

408 To apply the bELISA in the diagnosis of clinical animals, serum and oropharyngeal
409 samples were collected from 3 dogs at a pet clinic in Illinois. Dog-1 was a 6-year-old, male
410 neutered, Samoyed. At the time (Feb 7, 2022) that samples were collected for SARS-CoV-2
411 tests, the dog had clinical signs of coughing and sneezing for about three weeks and was
412 tested positive for *Mycoplasma*. Dog-2 was a 5.5-month-old, male, Great Dane mix. The dog
413 started showing clinical signs of coughing, vomiting, decreased appetite, and extreme
414 lethargy in late January of 2022. Samples from Dog-2 were collected on February 7th for
415 testing. Dog-3 was 14-year-old, female sprayed, mixed breed dog, displaying coughing and
416 sneezing on March 3, 2022. She also had a history of airway disease. Samples were collected
417 on March 10, 2022.

418

419 **Procedure for blocking ELISA and indirect ELISA.** Both ELISAs were performed
420 using our previously described methods with modifications (21, 45). The bELISA could
421 detect antibodies from multiple animal species by allowing sample antibody binding to the
422 coated antigen on the ELISA plate first, followed by adding biotin-conjugated mAb. If
423 presence of anti-N antibodies in the animal serum, they will bind to the N antigen and block
424 the binding of biotinylated anti-N mAb to the N antigen. The mAb will be washed away and
425 no color signal will be developed in the subsequent steps. If there is no anti-N antibodies
426 present in the animal serum, the biotinylated anti-N mAb will bind to the N antigen, then the
427 HRP-conjugated streptavidin will be added and bind to the biotin that conjugated to mAb.
428 HRP substrate will be added to develop the color signal. Thus, the amount of anti-N
429 antibodies in the testing sample is inversely proportional to the level of color signal. To
430 conduct the bELISA test, initially, the odd number columns in Immulon 2HB plate (Thermo
431 Fisher Scientific, Waltham, MA, USA) were coated with recombinant N protein (175ng)

432 diluted in antigen coating buffer (ACB; 35 mM sodium bicarbonate and 15 mM sodium
433 carbonate, PH 8.8). The even number columns in the plate were added with ACB only as the
434 background control. The plate was incubated at 37°C for 1 hour and then 4°C overnight. After
435 blocking with 2% bovine serum albumin (BSA; Thermo Fisher Scientific, Waltham, MA,
436 USA) in PBST (0.05% Tween 20 in 1x phosphate-buffered saline) at 37°C for 1 hour, the
437 plate was washed three times by PBST using the automated microplate washer (BioTek,
438 Winooski, VT). The test serum samples were diluted 1:4 with 2% BSA and added into both
439 coated and uncoated wells. The internal control standards (100 ul; high-, medium-, low-
440 positive, and negative) were added in duplicates. After incubation for 1 hour at 37°C, 100 µL
441 of biotinylated mAb (clone #127-3) was added and incubated at 37°C for another 30 min. The
442 plate was washed for three times and incubated with 100 uL of streptavidin poly-HRP
443 (1:2000 dilution; Thermo Fisher Scientific, Waltham, MA) at room temperature for 1 hour.
444 After wash with PBST, 100 µL of ABTS peroxidase substrate (KPL, Gaithersburg, MD) was
445 added for color development. The colorimetric reaction was stopped by equal volume of
446 ABTS stop solution (KPL, Gaithersburg, MA) in 5 min and color intensity was quantified at
447 405 nm using a SpectraMax® iD5 microplate reader (Molecular Devices, San Jose, CA). The
448 percentage of inhibition was calculated using the following formula:

$$449 \text{ Percent Inhibition (PI)} = \left(1 - \frac{A_{405} \text{ of sample} - A_{405} \text{ of ACB}}{A_{405} \text{ of negative control}} \right) * 100$$

450

451 For indirect ELISA, the plate was coated using the same method as that of bELISA. After
452 blocking with 5% non-fat milk in PBST, serum samples (1:400 dilution in 5% non-fat milk)
453 and internal control standards were loaded on the plate and incubated at 37°C for 1 hour. The
454 plate was washed for three times and then added 100 uL of HRP-conjugated goat anti-feline
455 IgG (H+L) secondary antibody (1:5000 dilution; Thermo Fisher Scientific, Waltham, MA) for
456 incubation another hour at 37°C. After washing of the plate, colorimetric reaction was
457 developed by adding ABTS peroxidase substrate and stopped by ABTS stop solution. Color
458 development was quantified using the SpectraMax® iD5 microplate reader (Molecular
459 Devices, San Jose, CA).

460

461 **Validation of N protein-based blocking ELISA.** For analytical sensitivity analysis of
462 the bELISA, two-fold serial dilutions of the high-positive and negative serum standards were
463 tested in triplicate and differences between different dilutions of the control serum were
464 evaluated by one-way analysis of variance (ANOVA) using Prism software version 6
465 (GraphPad Software, San Diego, California). A *p*-value of less than 0.01 (**) was considered
466 as statistically significant.

467 To determine the optimal diagnostic sensitivity and specificity, the four sets of known-
468 status animals serum samples mentioned above were subject to bELISA test. Calculations of
469 the assay performance were conducted using MedCalc®, version 10.4.0.0 (MedCalc®
470 Software, Mariarke, Belgium). The cutoff of bELISA was defined as the PI value that was
471 able to produce the maximized diagnostic sensitivity and specificity. In addition, Receiver
472 operating characteristic (ROC) analysis was performed using the same software to assess the

473 overall accuracy of the assay.

474 The assay repeatability was determined by running repeated samples of the medium-
 475 positive control. Assay precisions were calculated as 40 replicates in one plate for within-
 476 plate level, 3 plates in one run for between-plate level, and 3 consecutive runs for between-
 477 run level. Means, standard deviations, and percent coefficient of variation (%CV) values were
 478 calculated using Control Chart Pro Plus software (ChemSW, Inc., Fairfield Bay, AR, USA).

479

480 ACKNOWLEDGMENTS

481 We thank Dr. Mia K. Torchetti from USDA National Veterinary Services Laboratories for
 482 testing the dog samples. This project was supported by the National Institute of Health
 483 (Grant# R01AI166791). Fangfeng Yuan was partially supported by Illinois Distinguished
 484 Fellowship for graduate student at the University of Illinois.

485

486 **Table1. Reactivity of mAbs with different SARS-CoV-2 variants**

mAb clone#	B.1	WA1	P.1	B.1.1.7	B.1.617.2
41-10	++	++	++	++	++
86-12	++	++	++	++	++
109-33	+	+	+	+	+
127-3	+++	+++	+++	+++	+++
B6G11	+++	+++	+++	+++	+++

487 “+” weak reactivity, “++” moderate reactivity, “+++” strong reactivity.

488

489 **Table 2. Cross-reactivity of mAbs with other coronaviruses**

mAb clone #	SARS-CoV	MERS-CoV	HCoV OC43	HCoV NL63	HCoV 229E	HCoV HKU1	FCoV	FIPV	CCoV - type I	CCoV - type II	Ferret CoV	Mink CoV
86-12	+	-	-	+	-	-	-	-	+	-	-	-
127-3	-	-	-	-	-	-	-	-	-	-	-	-
41-10	-	-	-	-	-	-	-	-	-	-	-	-
109-33	-	-	-	-	-	-	-	-	-	-	-	-
B6G11	+	-	-	-	-	-	-	-	-	-	-	-

490

491

492

493 **FIGURE LEGEND**

494 **Figure 1. SARS-CoV-2 N antigen preparation and mAb characterization. (A)**

495 Recombinant N antigen expression and detection. Left panel, SDS-PAGE gel electrophoresis
496 of recombinant N protein, followed by Coomassie blue staining; right panel, Western blot
497 detection of His-tagged N protein. The membrane was stained with anti-His tag antibody. **(B)**
498 IFA detection of the N protein expressed in transfected MARC-145 cells. Fixed cells were
499 stained by the corresponding mAb and FITC-conjugated goat anti-mouse IgG was used as the
500 secondary antibody. Nuclei were counterstained with DAPI (blue). **(C)** MAb reactivity tested
501 on Western blot and immunoprecipitation (IP). Lysates from transfected 293T cells
502 expressing the N protein were harvested and utilized for WB and IP analysis.

503 **Figure 2. Establish positive and negative control standards.** A set of internal control
504 serum standards was prepared using experimental cat serum and assayed by indirect ELISA
505 **(A)** and blocking ELISA **(B)**. X-axis represents the positive and negative controls. Y-axis
506 shows the OD₄₀₅ for indirect ELISA and PI for bELISA. Each control standard was
507 highlighted in different colors and mean value was displayed on top of each column.

508 **Figure 3. Analytical sensitivity of bELISA.** Two-fold serial dilutions of the high-positive
509 and negative cat serum control standards were run in parallel. Each dilution was tested in
510 duplicates. OD values **(A)** or percentage of inhibition (PI) values **(B)** were calculated and
511 displayed in Y-axis. Differences under each dilution were analyzed by one-way analysis of
512 variance (ANOVA) using GraphPad Prism 6 software (GraphPad, La Jolla, CA). P-values
513 were indicated by asterisks. ** P < 0.01, *** P < 0.001.

514 **Figure 4. Determination of diagnostic sensitivity and specificity.** Receiver operating
515 characteristic (ROC) analysis **(A)** and the interactive plot of diagnostic sensitivity and
516 specificity **(B)** were calculated using 45 known-positive serum samples and 88 known-
517 negative serum samples collected from different animal species, including cat, ferret, mink,
518 and deer. A horizontal line between the positive and negative populations in panel A
519 represents the cutoff value that produces the optimal diagnostic sensitivity and specificity.
520 ROC analysis was conducted by using MedCalc software (version 10.4.0.0, MedCalc
521 Software, Mariarke, Belgium).

522 **Figure 5. Dynamics of antibody response in cats infected by different SARS-CoV-2**
523 **variants.** A total of 24 domestic cats were divided into four groups, in which each group was
524 inoculated with one of the SARS-CoV-2 variants (B.1, Delta, Omicron) and group four was
525 mock-inoculated with cell culture medium. Serum samples were collected before infection
526 and 3, 5, 7, 17 days post infection (DPI). **(A)** bELISA test to measure the antibody response
527 through the time course study. The dashed line represents the cutoff value (17.60%) of the
528 assay. **(B)** Serum neutralization assay. The assay was performed using SARS-CoV-2 Delta
529 variant (B.1.617.2). Neutralizing antibody titer was calculated as the reciprocal of the highest
530 serum dilution that generated 100% neutralization of SARS-CoV-2 infection. Statistical
531 differences between each group within each time point were calculated using one-way
532 analysis of variance (ANOVA). * P < 0.05, ** P < 0.01.

533 **Figure 6. Detection of SARS-CoV-2 specific antibody response in dogs with clinical**
534 **diseases. (A)** Serum samples from three dogs were tested by bELISA and sVNT. bELISA
535 results were presented in blue bar, while sVNT results were presented in orange bar. X-axis
536 shows individual dogs and values for both assays were presented on top of column. **(B)**
537 Serum antibody titers in Dog 2 tested by bELISA through a time course study. Dashed lines
538 represent the cut-off values for bELISA (17.60%) and sVNT (30%).

539 **REFERENCES**

- 540 1. Rambaut A, Holmes EC, O’Toole Á, Hill V, McCrone JT, Ruis C, du Plessis L, Pybus
541 OG. 2020. A dynamic nomenclature proposal for SARS-CoV-2 lineages to assist
542 genomic epidemiology. *Nature Microbiology* 5:1403-1407.
- 543 2. Enjuanes L, Gorbalenya AE, de Groot RJ, Cowley JA, Ziebuhr J, Snijder EJ. 2008.
544 Nidovirales. *Encyclopedia of Virology* doi:10.1016/B978-012374410-4.00775-5:419-
545 430.
- 546 3. V’kovski P, Kratzel A, Steiner S, Stalder H, Thiel V. 2021. Coronavirus biology and
547 replication: implications for SARS-CoV-2. *Nature Reviews Microbiology* 19:155-
548 170.
- 549 4. Heffron AS, McIlwain SJ, Amjadi MF, Baker DA, Khullar S, Armbrust T, Halfmann
550 PJ, Kawaoka Y, Sethi AK, Palmenberg AC, Shelef MA, O’Connor DH, Ong IM.
551 2021. The landscape of antibody binding in SARS-CoV-2 infection. *PLOS Biology*
552 19:e3001265.
- 553 5. Damas J, Hughes GM, Keough KC, Painter CA, Persky NS, Corbo M, Hiller M,
554 Koepfli K-P, Pfenning AR, Zhao H, Genereux DP, Swofford R, Pollard KS, Ryder
555 OA, Nweeia MT, Lindblad-Toh K, Teeling EC, Karlsson EK, Lewin HA. 2020. Broad
556 host range of SARS-CoV-2 predicted by comparative and structural analysis of ACE2
557 in vertebrates. *Proceedings of the National Academy of Sciences* 117:22311.
- 558 6. Sailleau C, Dumarest M, Vanhomwegen J, Delaplace M, Caro V, Kwasiborski A,
559 Hourdel V, Chevaillier P, Barbarino A, Comtet L, Pourquier P, Klonjowski B,

- 560 Manuguerra J-C, Zientara S, Le Poder S. 2020. First detection and genome
561 sequencing of SARS-CoV-2 in an infected cat in France. *Transboundary and*
562 *emerging diseases* 67:2324-2328.
- 563 7. McAloose D, Laverack M, Wang L, Killian Mary L, Caserta Leonardo C, Yuan F,
564 Mitchell Patrick K, Queen K, Mauldin Matthew R, Cronk Brittany D, Bartlett Susan
565 L, Sykes John M, Zec S, Stokol T, Ingerman K, Delaney Martha A, Fredrickson R,
566 Ivančić M, Jenkins-Moore M, Mazingo K, Franzen K, Bergeson Nichole H, Goodman
567 L, Wang H, Fang Y, Olmstead C, McCann C, Thomas P, Goodrich E, Elvinger F,
568 Smith David C, Tong S, Slavinski S, Calle Paul P, Terio K, Torchetti Mia K, Diel
569 Diego G, Meng X-J. From People to Panthera: Natural SARS-CoV-2 Infection in
570 Tigers and Lions at the Bronx Zoo. *mBio* 11:e02220-20.
- 571 8. Sharun K, Tiwari R, Saied AA, Dhama K. 2021. SARS-CoV-2 vaccine for domestic
572 and captive animals: An effort to counter COVID-19 pandemic at the human-animal
573 interface. *Vaccine* 39:7119-7122.
- 574 9. Chandler JC, Bevins SN, Ellis JW, Linder TJ, Tell RM, Jenkins-Moore M, Root JJ,
575 Lenoche JB, Robbe-Austerman S, DeLiberto TJ, Gidlewski T, Kim Torchetti M,
576 Shriner SA. 2021. SARS-CoV-2 exposure in wild white-tailed deer
577 (*Odocoileus virginianus*). *Proceedings of the National*
578 *Academy of Sciences* 118:e2114828118.
- 579 10. Oreshkova N, Molenaar RJ, Vreman S, Harders F, Oude Munnink BB, Hakze-van der
580 Honing RW, Gerhards N, Tolsma P, Bouwstra R, Sikkema RS, Tacke MG, de Rooij

- 581 MM, Weesendorp E, Engelsma MY, Brusckke CJ, Smit LA, Koopmans M, van der
582 Poel WH, Stegeman A. 2020. SARS-CoV-2 infection in farmed minks, the
583 Netherlands, April and May 2020. Euro surveillance : bulletin Europeen sur les
584 maladies transmissibles = European communicable disease bulletin 25:2001005.
- 585 11. Medkour H, Catheland S, Boucraut-Baralon C, Laidoudi Y, Sereme Y, Pingret J-L,
586 Million M, Houhamdi L, Levasseur A, Cabassu J, Davoust B. 2021. First evidence of
587 human-to-dog transmission of SARS-CoV-2 B.1.160 variant in France.
588 Transboundary and emerging diseases doi:10.1111/tbed.14359:10.1111/tbed.14359.
- 589 12. Barroso-Arévalo S, Rivera B, Domínguez L, Sánchez-Vizcaíno JM. 2021. First
590 Detection of SARS-CoV-2 B.1.1.7 Variant of Concern in an Asymptomatic Dog in
591 Spain. Viruses 13:1379.
- 592 13. Kevadiya BD, Machhi J, Herskovitz J, Oleynikov MD, Blomberg WR, Bajwa N, Soni
593 D, Das S, Hasan M, Patel M, Senan AM, Gorantla S, McMillan J, Edagwa B,
594 Eisenberg R, Gurumurthy CB, Reid SPM, Punyadeera C, Chang L, Gendelman HE.
595 2021. Diagnostics for SARS-CoV-2 infections. Nature materials 20:593-605.
- 596 14. Deeks JJ, Dinnes J, Takwoingi Y, Davenport C, Spijker R, Taylor-Phillips S, Adriano
597 A, Beese S, Dretzke J, Ferrante di Ruffano L, Harris IM, Price MJ, Dittrich S,
598 Emperador D, Hooft L, Leeftang MM, Van den Bruel A, Cochrane C-DTAG. 2020.
599 Antibody tests for identification of current and past infection with SARS-CoV-2. The
600 Cochrane database of systematic reviews 6:CD013652-CD013652.
- 601 15. Liu K-T, Han Y-J, Wu G-H, Huang K-YA, Huang P-N. 2022. Overview of

- 602 Neutralization Assays and International Standard for Detecting SARS-CoV-2
- 603 Neutralizing Antibody. *Viruses* 14:1560.
- 604 16. Fenwick C, Turelli P, Pellaton C, Farina A, Campos J, Raclot C, Pojer F, Cagno V,
605 Nusslé SG, D'Acremont V, Fehr J, Puhan M, Pantaleo G, Trono D. 2021. A high-
606 throughput cell- and virus-free assay shows reduced neutralization of SARS-CoV-2
607 variants by COVID-19 convalescent plasma. *Science Translational Medicine*
608 13:eabi8452.
- 609 17. Henriques AM, Fagulha T, Barros SC, Ramos F, Duarte M, Luís T, Fevereiro M.
610 2016. Development and validation of a blocking ELISA test for the detection of avian
611 influenza antibodies in poultry species. *Journal of Virological Methods* 236:47-53.
- 612 18. Ferrin NH, Fang Y, Johnson CR, Murtaugh MP, Polson DD, Torremorell M, Gramer
613 ML, Nelson EA. 2004. Validation of a blocking enzyme-linked immunosorbent assay
614 for detection of antibodies against porcine reproductive and respiratory syndrome
615 virus. *Clinical and diagnostic laboratory immunology* 11:503-514.
- 616 19. Martins M, do Nascimento Gabriela M, Nooruzzaman M, Yuan F, Chen C, Caserta
617 Leonardo C, Miller Andrew D, Whittaker Gary R, Fang Y, Diel Diego G. 2022. The
618 Omicron Variant BA.1.1 Presents a Lower Pathogenicity than B.1 D614G and Delta
619 Variants in a Feline Model of SARS-CoV-2 Infection. *Journal of Virology* 96:e00961-
620 22.
- 621 20. Carvallo FR, Martins M, Joshi LR, Caserta LC, Mitchell PK, Cecere T, Hancock S,
622 Goodrich EL, Murphy J, Diel DG. 2021. Severe SARS-CoV-2 Infection in a Cat with

- 623 Hypertrophic Cardiomyopathy. *Viruses*. 13(8):doi:10.3390/v13081510.
- 624 21. Yuan F, Petrovan V, Gimenez-Lirola LG, Zimmerman JJ, Rowland RRR, Fang Y.
625 2021. Development of a Blocking Enzyme-Linked Immunosorbent Assay for
626 Detection of Antibodies against African Swine Fever Virus. *Pathogens* 10.
- 627 22. Olival KJ, Cryan PM, Amman BR, Baric RS, Blehert DS, Brook CE, Calisher CH,
628 Castle KT, Coleman JTH, Daszak P, Epstein JH, Field H, Frick WF, Gilbert AT,
629 Hayman DTS, Ip HS, Karesh WB, Johnson CK, Kading RC, Kingston T, Lorch JM,
630 Mendenhall IH, Peel AJ, Phelps KL, Plowright RK, Reeder DM, Reichard JD,
631 Sleeman JM, Streicker DG, Towner JS, Wang L-F. 2020. Possibility for reverse
632 zoonotic transmission of SARS-CoV-2 to free-ranging wildlife: A case study of bats.
633 *PLOS Pathogens* 16:e1008758.
- 634 23. Prince T, Smith SL, Radford AD, Solomon T, Hughes GL, Patterson EI. 2021. SARS-
635 CoV-2 Infections in Animals: Reservoirs for Reverse Zoonosis and Models for Study.
636 *Viruses* 13:494.
- 637 24. Goraichuk IV, Arefiev V, Stegnyy BT, Gerilovych AP. 2021. Zoonotic and Reverse
638 Zoonotic Transmissibility of SARS-CoV-2. *Virus research* 302:198473-198473.
- 639 25. Ainsworth M, Andersson M, Auckland K, Baillie JK, Barnes E, Beer S, Beveridge A,
640 Bibi S, Blackwell L, Borak M, Bown A, Brooks T, Burgess-Brown NA, Camara S,
641 Catton M, Chau KK, Christott T, Clutterbuck E, Coker J, Cornall RJ, Cox S,
642 Crawford-Jones D, Crook DW, D'Arcangelo S, Dejnirattasai W, Dequaire JMM,
643 Dimitriadis S, Dingle KE, Doherty G, Dold C, Dong T, Dunachie SJ, Ebner D,

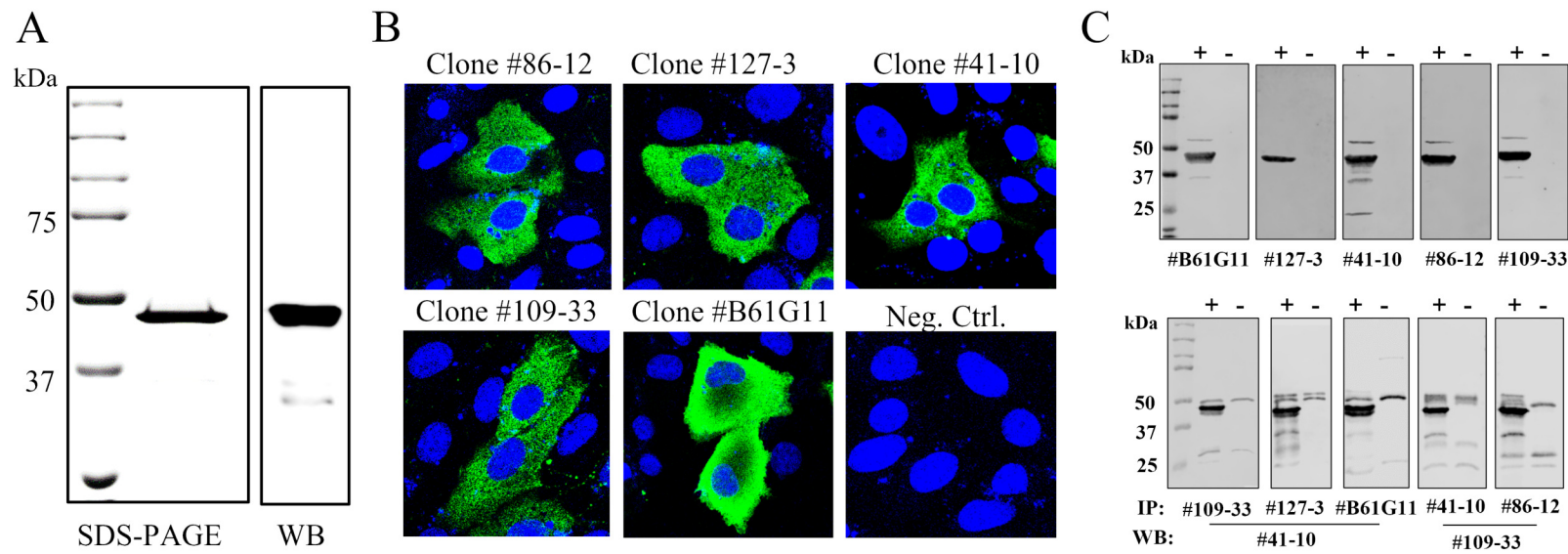
- 644 Emmenegger M, Espinosa A, Eyre DW, Fairhead R, Fassih S, Feehily C, Felle S,
645 Fernandez-Cid A, Fernandez Mendoza M, Foord TH, Fordwoh T, Fox McKee D,
646 Frater J, Gallardo Sanchez V, Gent N, Georgiou D, Groves CJ, et al. 2020.
647 Performance characteristics of five immunoassays for SARS-CoV-2: a head-to-head
648 benchmark comparison. *The Lancet Infectious Diseases* 20:1390-1400.
- 649 26. Tan CW, Chia WN, Qin X, Liu P, Chen MIC, Tiu C, Hu Z, Chen VC-W, Young BE,
650 Sia WR, Tan Y-J, Foo R, Yi Y, Lye DC, Anderson DE, Wang L-F. 2020. A SARS-
651 CoV-2 surrogate virus neutralization test based on antibody-mediated blockage of
652 ACE2–spike protein–protein interaction. *Nature Biotechnology* 38:1073-1078.
- 653 27. Mehdi F, Chattopadhyay S, Thiruvengadam R, Yadav S, Kumar M, Sinha SK,
654 Goswami S, Kshetrapal P, Wadhwa N, Chandramouli Natchu U, Sopory S, Koundinya
655 Desiraju B, Pandey AK, Das A, Verma N, Sharma N, Sharma P, Bhartia V, Gosain M,
656 Lodha R, Lamminmäki U, Shrivastava T, Bhatnagar S, Batra G. 2021. Development
657 of a Fast SARS-CoV-2 IgG ELISA, Based on Receptor-Binding Domain, and Its
658 Comparative Evaluation Using Temporally Segregated Samples From RT-PCR
659 Positive Individuals. *Frontiers in Microbiology* 11.
- 660 28. Li T, Wang L, Wang H, Li X, Zhang S, Xu Y, Wei W. 2020. Serum SARS-COV-2
661 Nucleocapsid Protein: A Sensitivity and Specificity Early Diagnostic Marker for
662 SARS-COV-2 Infection. *Frontiers in Cellular and Infection Microbiology* 10:470.
- 663 29. Fenwick C, Croxatto A, Coste Alix T, Pojer F, André C, Pellaton C, Farina A, Campos
664 J, Hacker D, Lau K, Bosch B-J, Gonseth Nussle S, Bochud M, D’Acremont V, Trono

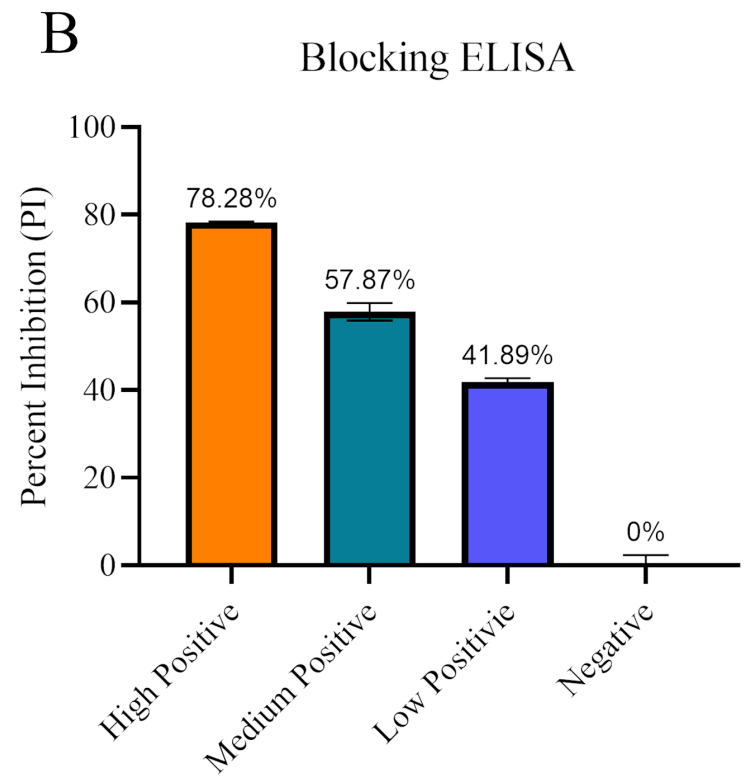
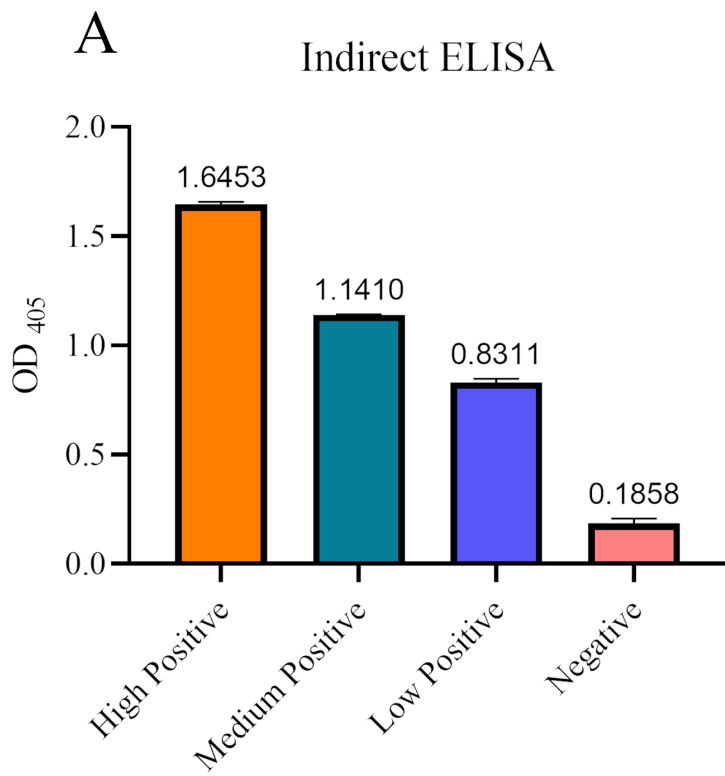
- 665 D, Greub G, Pantaleo G, Subbarao K. Changes in SARS-CoV-2 Spike versus
666 Nucleoprotein Antibody Responses Impact the Estimates of Infections in Population-
667 Based Seroprevalence Studies. *Journal of Virology* 95:e01828-20.
- 668 30. Mariën J, Ceulemans A, Michiels J, Heyndrickx L, Kerkhof K, Foque N, Widdowson
669 M-A, Mortgat L, Duysburgh E, Desombere I, Jansens H, Van Esbroeck M, Ariën KK.
670 2021. Evaluating SARS-CoV-2 spike and nucleocapsid proteins as targets for
671 antibody detection in severe and mild COVID-19 cases using a Luminex bead-based
672 assay. *Journal of Virological Methods* 288:114025.
- 673 31. Burbelo PD, Riedo FX, Morishima C, Rawlings S, Smith D, Das S, Strich JR,
674 Chertow DS, Davey RT, Jr., Cohen JI. 2020. Detection of Nucleocapsid Antibody to
675 SARS-CoV-2 is More Sensitive than Antibody to Spike Protein in COVID-19
676 Patients. *medRxiv : the preprint server for health sciences*
677 doi:10.1101/2020.04.20.20071423:2020.04.20.20071423.
- 678 32. Thudium Rebekka F, Stoico Malene P, Høgdall E, Høgh J, Krarup Henrik B, Larsen
679 Margit AH, Madsen Poul H, Nielsen Susanne D, Ostrowski Sisse R, Palombini A,
680 Rasmussen Daniel B, Foged Niels T, Caliendo Angela M. Early Laboratory Diagnosis
681 of COVID-19 by Antigen Detection in Blood Samples of the SARS-CoV-2
682 Nucleocapsid Protein. *Journal of Clinical Microbiology* 59:e01001-21.
- 683 33. Le Hingrat Q, Visseaux B, Laouenan C, Tubiana S, Bouadma L, Yazdanpanah Y,
684 Duval X, Burdet C, Ichou H, Damond F, Bertine M, Benmalek N, Choquet C, Timsit
685 J-F, Ghosn J, Charpentier C, Descamps D, Houhou-Fidouh N, Diallo A, Le Mestre S,

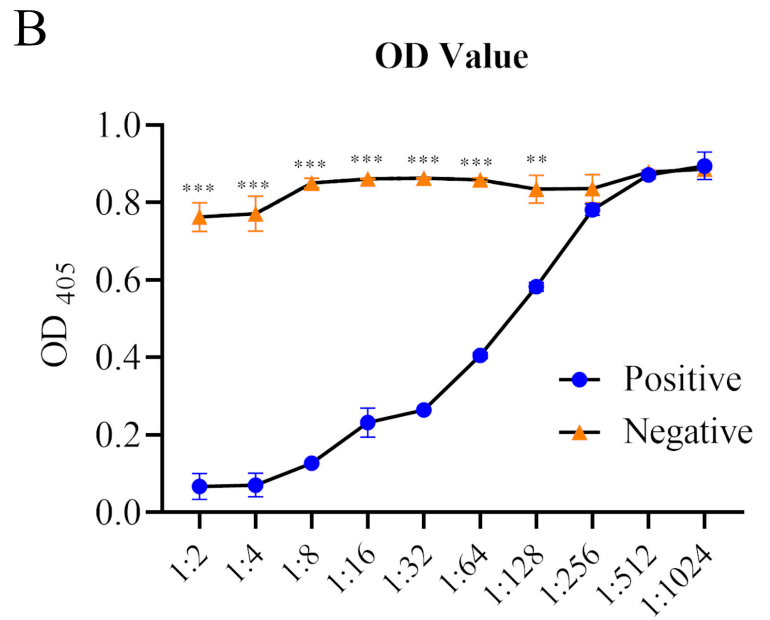
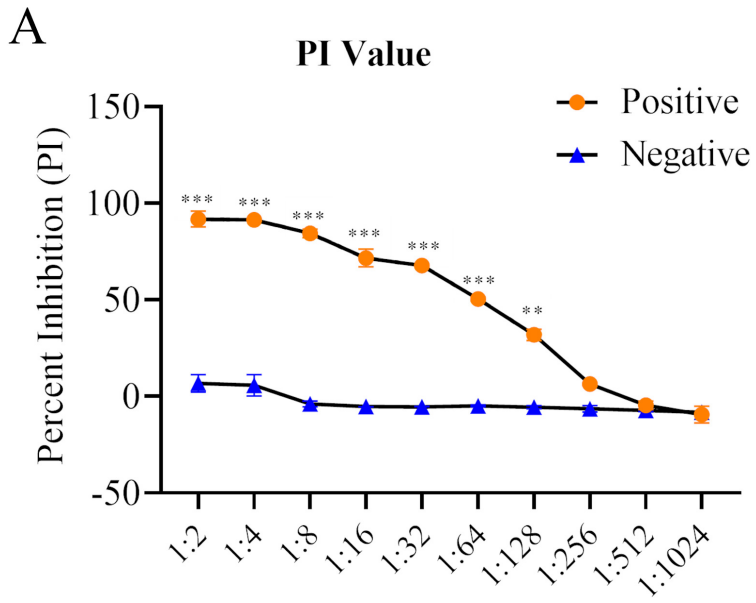
- 686 Mercier N, Paul C, Petrov-Sanchez V, Malvy D, Chirouze C, Andrejak C, Dubos F,
687 Rossignol P, Picone O, Bompard F, Gigante T, Gilg M, Rossignol B, Levy-Marchal C,
688 Beluze M, Hulot JS, Bachelet D, Bhavsar K, Bouadma L, Chair A, Couffignal C, Da
689 Silveira C, Debray MP, Descamps D, Duval X, Eloy P, Esposito-Farese M, Ettalhaoui
690 N, Gault N, Ghosn J, et al. 2021. Detection of SARS-CoV-2 N-antigen in blood
691 during acute COVID-19 provides a sensitive new marker and new testing alternatives.
692 *Clinical Microbiology and Infection* 27:789.e1-789.e5.
- 693 34. Li T, Wang L, Wang H, Li X, Zhang S, Xu Y, Wei W. 2020. Serum SARS-COV-2
694 Nucleocapsid Protein: A Sensitivity and Specificity Early Diagnostic Marker for
695 SARS-COV-2 Infection. *Frontiers in cellular and infection microbiology* 10:470-470.
- 696 35. Di B, Hao W, Gao Y, Wang M, Wang Y-d, Qiu L-w, Wen K, Zhou D-h, Wu X-w, Lu
697 E-j. 2005. Monoclonal antibody-based antigen capture enzyme-linked immunosorbent
698 assay reveals high sensitivity of the nucleocapsid protein in acute-phase sera of severe
699 acute respiratory syndrome patients. *Clinical and Vaccine Immunology* 12:135-140.
- 700 36. Lu X, Wang L, Sakthivel SK, Whitaker B, Murray J, Kamili S, Lynch B, Malapati L,
701 Burke SA, Harcourt J, Tamin A, Thornburg NJ, Villanueva JM, Lindstrom S. 2020.
702 US CDC Real-Time Reverse Transcription PCR Panel for Detection of Severe Acute
703 Respiratory Syndrome Coronavirus 2. *Emerging infectious diseases* 26:1654-1665.
- 704 37. Li K, Huang B, Wu M, Zhong A, Li L, Cai Y, Wang Z, Wu L, Zhu M, Li J, Wang Z,
705 Wu W, Li W, Bosco B, Gan Z, Qiao Q, Wu J, Wang Q, Wang S, Xia X. 2020.
706 Dynamic changes in anti-SARS-CoV-2 antibodies during SARS-CoV-2 infection and

- 707 recovery from COVID-19. *Nature Communications* 11:6044.
- 708 38. Wang H, Yuan Y, Xiao M, Chen L, Zhao Y, Haiwei Z, Long P, Zhou Y, Xu X, Lei Y,
709 Bihao W, Diao T, Cai H, Liu L, Shao Z, Wang J, Bai Y, Wang K, Peng M, Liu L, Han
710 S, Mei F, Cai K, Lei Y, Pan A, Wang C, Gong R, Li X, Wu T. 2021. Dynamics of the
711 SARS-CoV-2 antibody response up to 10 months after infection. *Cellular &*
712 *Molecular Immunology* 18:1832-1834.
- 713 39. Gaebler C, Wang Z, Lorenzi JCC, Muecksch F, Finkin S, Tokuyama M, Cho A,
714 Jankovic M, Schaefer-Babajew D, Oliveira TY, Cipolla M, Viant C, Barnes CO, Bram
715 Y, Breton G, Hägglöf T, Mendoza P, Hurley A, Turroja M, Gordon K, Millard KG,
716 Ramos V, Schmidt F, Weisblum Y, Jha D, Tankelevich M, Martinez-Delgado G, Yee J,
717 Patel R, Dizon J, Unson-O'Brien C, Shimeliovich I, Robbiani DF, Zhao Z, Gazumyan
718 A, Schwartz RE, Hatzioannou T, Bjorkman PJ, Mehandru S, Bieniasz PD, Caskey M,
719 Nussenzweig MC. 2021. Evolution of antibody immunity to SARS-CoV-2. *Nature*
720 591:639-644.
- 721 40. Peng P, Hu J, Deng H-j, Liu B-z, Fang L, Wang K, Tang N, Huang A-l. 2021. Changes
722 in the humoral immunity response in SARS-CoV-2 convalescent patients over 8
723 months. *Cellular & Molecular Immunology* 18:490-491.
- 724 41. Mibayashi M, Martínez-Sobrido L, Loo Y-M, Cárdenas WB, Gale M, Jr., García-
725 Sastre A. 2007. Inhibition of retinoic acid-inducible gene I-mediated induction of beta
726 interferon by the NS1 protein of influenza A virus. *Journal of virology* 81:514-524.
- 727 42. Petrovan V, Yuan F, Li Y, Shang P, Murgia MV, Misra S, Rowland RRR, Fang Y.

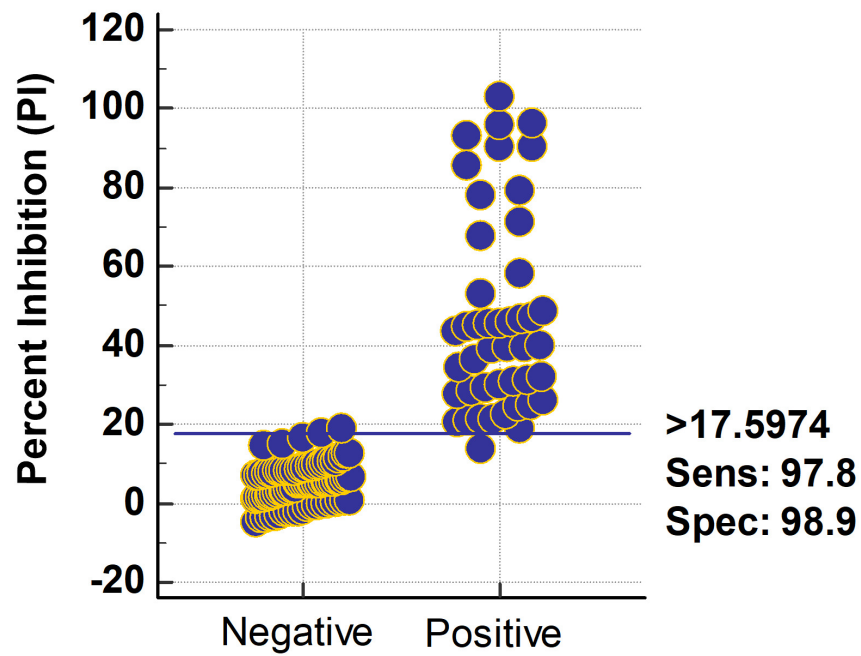
- 728 2019. Development and characterization of monoclonal antibodies against p30 protein
729 of African swine fever virus. *Virus Res* 269:197632.
- 730 43. Martins M, Fernandes Maureen HV, Joshi Lok R, Diel Diego G, Gallagher T. 2022.
731 Age-Related Susceptibility of Ferrets to SARS-CoV-2 Infection. *Journal of Virology*
732 96:e01455-21.
- 733 44. Palmer Mitchell V, Martins M, Falkenberg S, Buckley A, Caserta Leonardo C,
734 Mitchell Patrick K, Cassmann Eric D, Rollins A, Zylich Nancy C, Renshaw Randall
735 W, Guarino C, Wagner B, Lager K, Diel Diego G, Gallagher T. 2021. Susceptibility of
736 White-Tailed Deer (*Odocoileus virginianus*) to SARS-CoV-2. *Journal of Virology*
737 95:e00083-21.
- 738 45. Brown E, Lawson S, Welbon C, Gnanandarajah J, Li J, Murtaugh MP, Nelson EA,
739 Molina RM, Zimmerman JJ, Rowland RR, Fang Y. 2009. Antibody response to
740 porcine reproductive and respiratory syndrome virus (PRRSV) nonstructural proteins
741 and implications for diagnostic detection and differentiation of PRRSV types I and II.
742 *Clin Vaccine Immunol* 16:628-35.
- 743



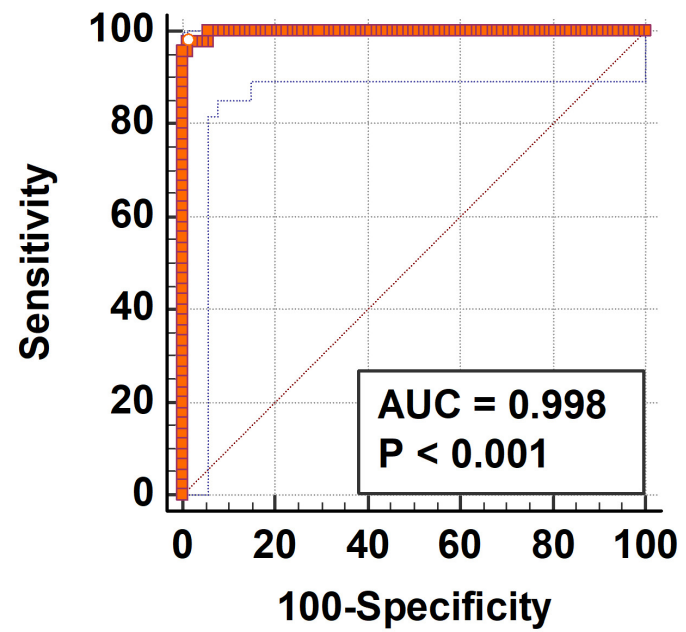




A

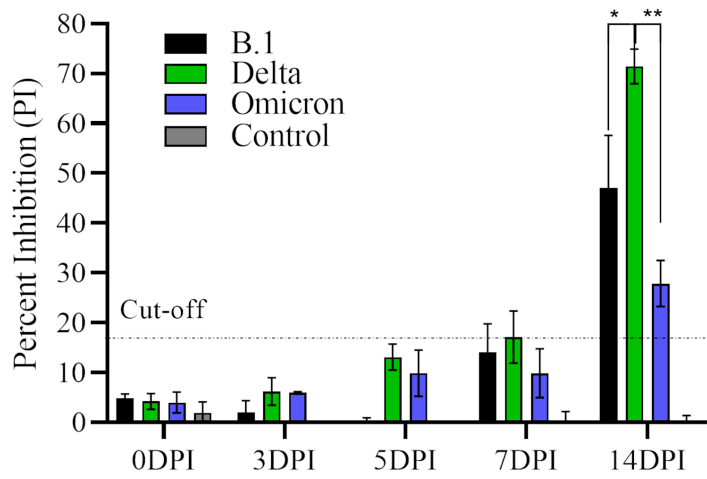


B



A

bELISA



B

SN

